Modelling of ice induced power losses and comparison with observations

presented at Winterwind 2011, February 8-10, Umeå, Sweden

Matthew C. Homola [a,b,1] Muhammad S. Virk [b]
Per J. Nicklasson [b] and Per A. Sundsbø [b]

[a] *Nordkraft Produksjon, Postboks 55, 8517 Narvik, Norway*

[b] *Department of Technology, Narvik University College Lodvelangesgate 2, Postboks 385, 8515 Narvik, Norway*

Abstract

Ice accretion along the blade of a large pitch controlled wind turbine (NREL 5 MW) was modelled using a CFD based solver. The aerodynamic properties were calculated using a CFD solver for both the ice free blade and the iced blade and a blade element momentum calculation was performed to determine the changes in the power curve resulting from the ice accretions. The modelled changes in the power curve were then compared with observed changes in power production for a similar, large, pitch controlled turbine when subject to icing. The modelled effects of icing were to found to be less severe than the observed, which can be due to the modelled results being generated with a shorter icing event than the observed one. The results are deemed to correspond reasonably well with the observed effects and give confidence that such modelling can be useful in estimating the effects of icing and exploring methods of reducing the adverse effects of icing.

1 Introduction

Wind power plants are increasingly being planned and built in areas where they are periodically subject to atmospheric icing. Many Arctic and Alpine regions have good wind resources, but icing on wind turbines has been recognized as a hinderance to the development of wind power in these regions. This icing, while being a danger to people in the vicinity of the turbine (Seifert, 2003) and increasing fatigue loads on the turbine (Ganander and Ronsten,

[1] tel: +47-76961636 email: matthew.homola@nordkraft.no

2003), also tends to degrade the aerodynamic performance of the blades resulting in potentially large power losses (Ronsten, 2004; Jasinski et al., 1998). The amount of energy production lost due to icing is an area of large uncertainty and this uncertainty a potential wind power investor must be paid for through a higher expected rate of return. The result is reduced investment due to the uncertainty.

Atmospheric icing causes power losses for wind turbines, due to instrument or controller errors caused by icing, and due to ice accumulations disrupting the blade (airfoil) aerodynamics. Previous work Virk et al. (2010); Homola et al. (2009) has indicated that for dry rime icing the icing becomes less significant for larger turbines, but the effect on energy production has not been fully investigated. The objective of this work was to use simulations to explore how atmospheric ice accretion along the length of a blade affects the energy production capabilities of a large standard wind turbine.

In this paper performance losses due to ice accretion on a 5 MW wind turbine blade were calculated using computational fluid dynamics based three-dimensional numerical simulations and blade element momentum (BEM) based analytical calculations, and the calculated reduction in power curve from the icing was then compared with measured results from icing events at Nygårdsfjell windpark.

2 Modelling the effect of icing

The NREL 5MW reference wind turbine (Jonkman et al., 2009) was selected as the test case for this study, because it is a large, variable speed, pitch controlled turbine design typical for current wind turbines and the complete design has been published. The NREL 5 MW wind turbine's blade radius used for this study is 63 meters long, and it was not practical to numerically simulate the icing on the whole blade, due to limited computational resources. Therefore five sections were selected along the blade radius, where each section was 0.5 meter wide. The selection of the tested sections was weighted towards the outer portion of the blade, as previous work has shown more ice on the outer half of the wind turbine blade (Antikainen et al., 2003; Antikainen and Peuranen, 2000). The sections and their locations on the complete blade are shown in Figure 1. These numerical analyses were carried out using an ice accretion solver 'FENSAP-ICE' from NTI (Newmerical, 2010). Each selected section along the blade has different geometric characteristics (chord length, twist angle, thickness to chord ratio).

The numerical simulations of the icing shapes were carried out at the operating conditions specified in Table 1. Following the calculation of the ice shapes, the

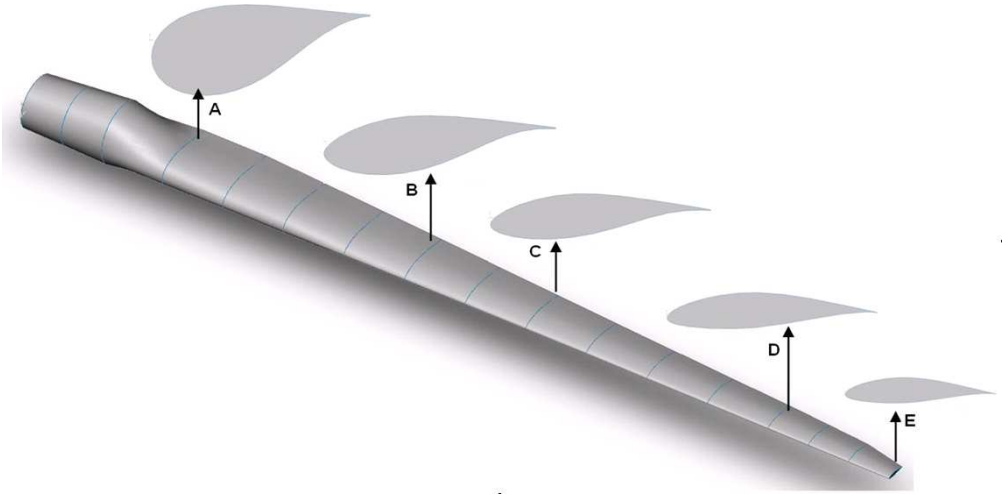

Fig. 1. 3D CAD of the NREL 5 MW wind turbine blade, showing the selected sections.

aerodynamic properties of the iced sections were found by calculating the lift and drag forces for varying angles of attack around the test sections normal operating angles.

Table 1
Modelled icing conditions.

Free stream wind velocity, V_{inf}, [m/s]	10
Droplet size, MVD [μm]	20
Liquid water content, LWC [g/m^3]	0.22
Air temperature [°C]	-10
Simulation time [min]	60

2.1 Aerodynamic coefficients

The aerodynamic coefficients of the clean and iced blade profiles were calculated using Navier-Stokes equations in FENSAP. The results obtained were compared with the data in the NREL report (Jonkman et al., 2009), which is for a clean blade, and a reasonable agreement was found in the range of normal operation. The NREL data was 2D measured coefficients corrected for rotational stall delay. The original coefficients are from Appendix A of DOWEC document 10046_009.pdf (Kooijman et al., 2003) and the NACA coefficients from Abbott and von Doenhoff (1959).

For the lift and drag analyses carried out in FENSAP, a simplification was done in that rotational effects on aerodynamic performance were not included. This causes an underestimation of the lift coefficient at the inner most section

(section A), but the influence of rotation depends on the span wise location along the blade (Van Rooij and Timmer, 2003) so this does not significantly affect the mid and outer sections. The inboard section is least significant in terms of power production so this simplification was deemed acceptable. Particularly as the difference due to the ice was the subject of study here and the same simplification was done for both the clean and iced profiles.

2.2 Blade element momentum calculations

The blade element momentum calculation was initially performed for the five clean sections to establish the baseline performance, and to determine the operating conditions at each section for the icing calculation. Thereafter BEM calculations were performed for the iced blade profile sections using the C_l and C_d values calculated from the computational fluid dynamics based numerical analyses, and using the C_l and C_d values in the NREL report (Jonkman et al., 2009). The BEM calculations were performed to determine the coefficient of performance (C_p) for the blade, and the results of these calculations are shown in Figure 2.

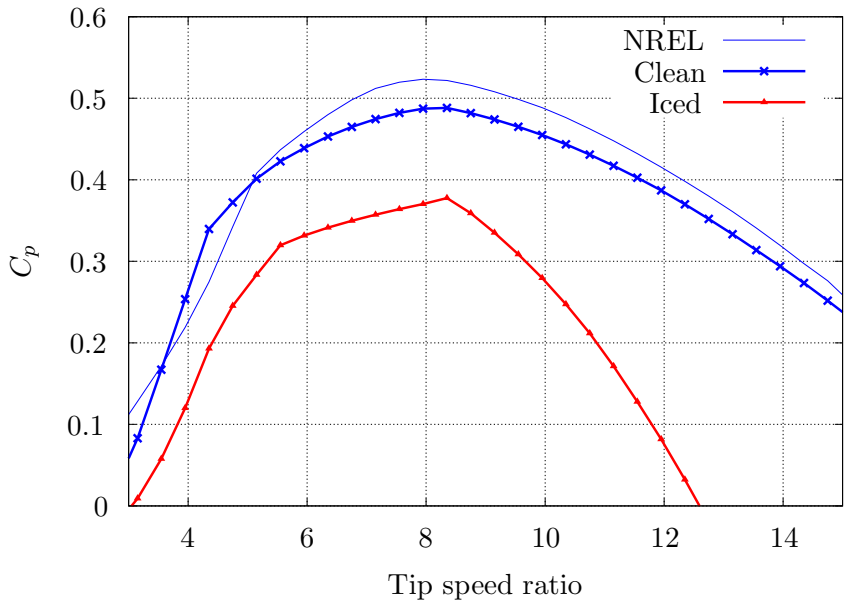

Fig. 2. Power coefficient vs. tip speed ratio from BEM analysis using blade aerodynamic data from NREL report, clean case and iced case.

2.3 Power coefficient

The power coefficient versus tip speed ratio calculated using the NREL lift and drag data, and the FENSAP lift and drag data for the clean and iced

blade cases are shown in Figure 2. The shapes are as expected for a modern three bladed wind turbine, with the peaks being around a tip speed ratio of 8. It can be seen that the maximum performance drops clearly with the ice shapes, from a peak of 0.49 for the clean case to a peak of 0.38 for the iced case. While the entire C_p curve for the iced case is lower than for the clean case, it can also be seen that the decrease is greatest at higher tip speed ratios, where the higher drag caused by the rough ice surface has more significance.

2.4 Power curves

The power curves for the clean case and for the iced case are shown in Figure 3, together with the curve published by NREL. The NREL curve is nearly indistinguishable from the clean case. It can be seen that there is a significant power loss of about 27% for control region two due to the icing.

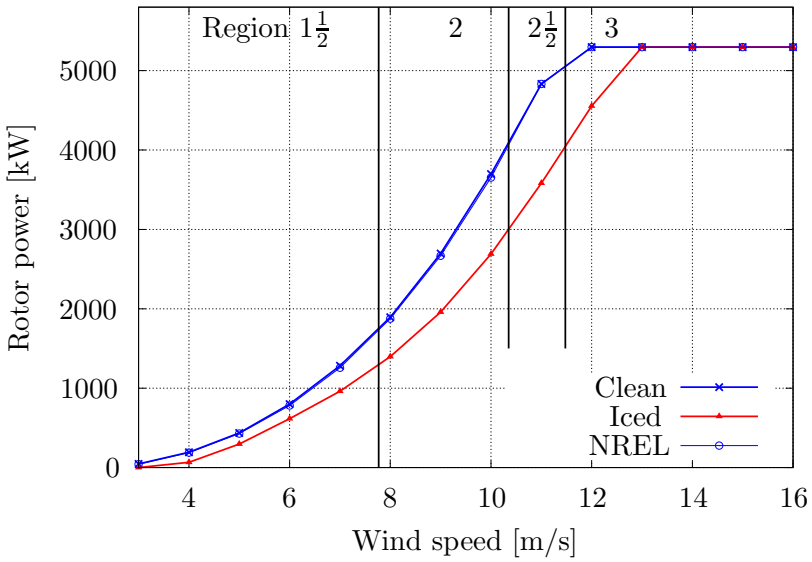

Fig. 3. Calculated power performance curves together with the published NREL curve. The control regions defined by NREL are also shown.

3 Measuring the effect of icing

Ideally the modelled turbine would have been the same as the actual turbines, but the turbine geometry and control parameters from the turbines at Nygårdsfjell were not available for this work. Therefor the 5 MW NREL reference turbine was used instead. The operation principle is the same for both the NREL turbine and the turbines at Nygårdsfjell. Both are modern, pitch

controlled, variable speed, multi-megawatt turbines. Finally, no measure of droplet size or liquid water content was performed at Nygårdsfjell, so those input parameters had to be assumed. The liquid water content and droplet size was chosen similarly to previous studies such that the results can be compared.

3.1 Power curves

To calculate the power curve performance of these wind turbines some filtering and pre data analysis was necessary. The measured power curves for the wind turbines are quite different for easterly and westerly winds, probably due to complex terrain around the site. Wind primarily blows from only those two directions, as can be seen in Figure 4, so a separate power curve was generated for each primary direction.

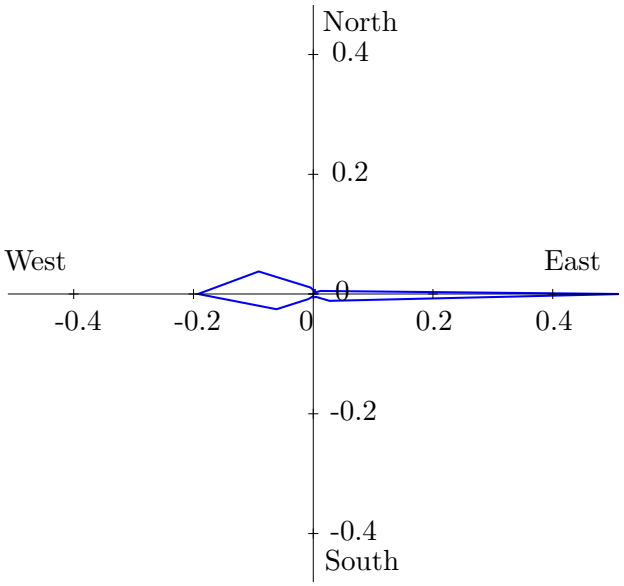

Fig. 4. Wind frequency radar plot showing the percentage of time the wind comes from different sectors. East and west are clearly the two dominant directions.

The power curves were generated by the following process. First, all periods during which the turbine was stopped were removed. Thereafter the data was binned using the wind speed, as described in the IEC standard (IEC 61400-12-1, 2005), using bins of 0.5 m/s. The wind speed was corrected for changes in density resulting from temperature changes according to the IEC standard.

The data in a bin consists of a spread of points. The spreading of the data is dependent on many factors, including: variations in wind speed, wind direction, wind shear, turbine misalignment, and uncertainty in the measurements of wind speed and output power. The spread of data points are reduced to one average wind speed and one average power production for each bin. This

spread of data points can be seen as a band of data points when the measured power production from a wind turbine is plotted relative to wind speed. The filtered production data used to generate the power curve for one direction of one of the wind turbines at Nygårdsfjell is shown together with the resulting calculated power curve in Figure 5.

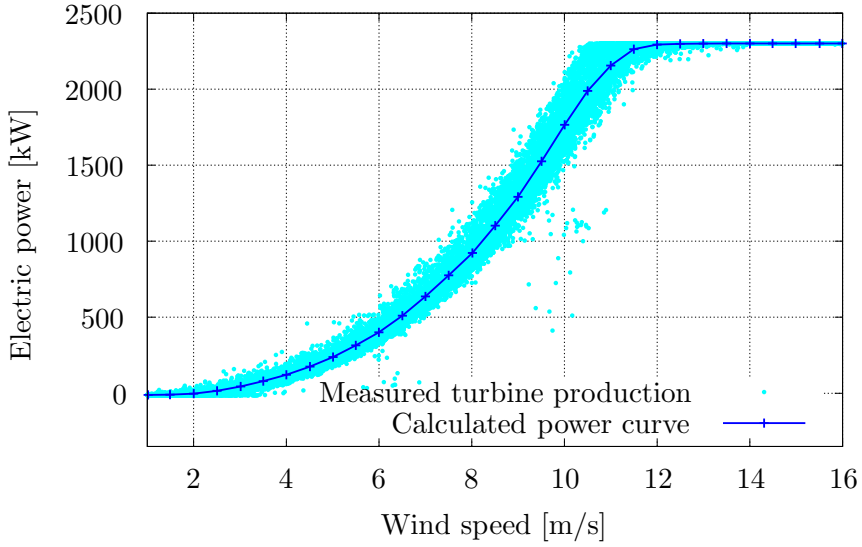

Fig. 5. All data used to generate a power curve for one direction and the resulting power curve.

3.2 Icing events and power production

Several periods of operation during icing conditions were identified during the 2008-2009 winter. Two of the periods are here described in more detail.

The first period was in the time frame December 5 - Dec. 9, 2008, with the main icing apparently occurring on December 5. During this icing period the cup anemometers were seen to slow and finally stop, while the ultrasonic anemometers were reporting nearly constant wind speed. Photographs from the fifth were not usable for identification of icing due to poor visibility, but photographs of the tail section of the nacelle from the sixth clearly show rime icing on the cup anemometer and lightning rods, as can be seen in Figure 6.

In Figure 7 the production can be seen to decrease at 8-10 m/s wind speed to much below the normal range of operation as the icing event progresses even as the wind speed is relatively unchanged. Production then ceases as the wind speed eventually decreases. When this is compared with the calculated power loss due to icing shown in Figure 3 it can be seen that the power production here gradually decreases below the modeled curve for the iced case. This is as expected for a turbine operating in icing conditions. For a certain build-up of

Fig. 6. Rime ice visible on the sensors following the icing event Dec. 5.

ice the turbine should operate as in the modeled ice case, and when the ice is further increased the performance should decrease further.

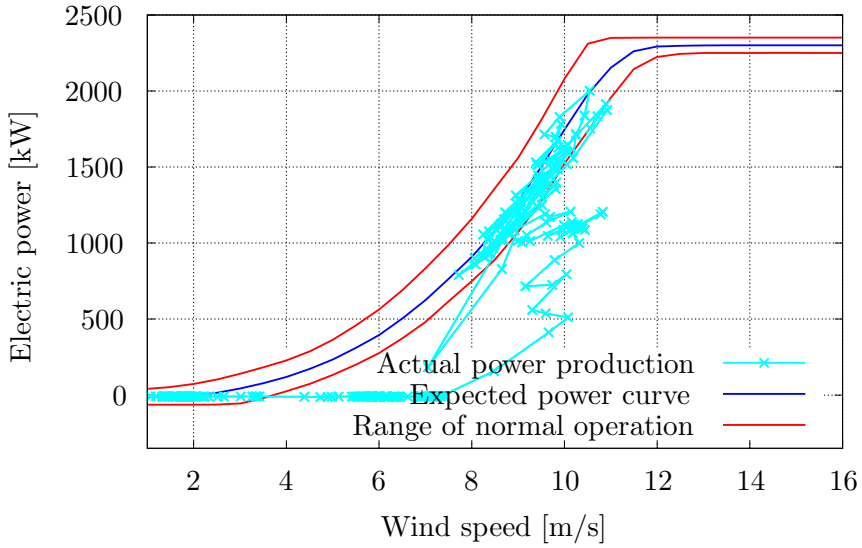

Fig. 7. Measured power production during the icing event of Dec. 5 (consecutive points are connected) can be seen to decrease from normal operation at 8-10 m/s wind speed to much below the normal range of operation as the icing event progresses even as the wind speed is relatively unchanged. Production then ceases as the wind speed eventually decreases.

The second period was in the time frame January 7 - January 10, 2009, with the main icing apparently occurring in the evening of January 8. Due to the event occurring at night, no pictures were able to show clearly any ice or lack thereof. In Figure 8 the production can be seen to remain below the range of normal operation as the wind speed increases from near 0 up to rated wind

speed. At about 20% over rated wind speed rated power is finally attained, and thereafter maintained. When this is compared with the calculated power loss due to icing shown in Figure 3 it can be seen that the power production here is initially much less than the modeled curve for the iced case, but then jumps up to nearly the modeled iced case, when the wind speed reached 8 m/s, and then varies about somewhat below the modeled ice case as wind speed increases. The jump in production is perhaps due to partial ice shedding from the blade, but unfortunately no observations exist to corroborate this hypothesis.

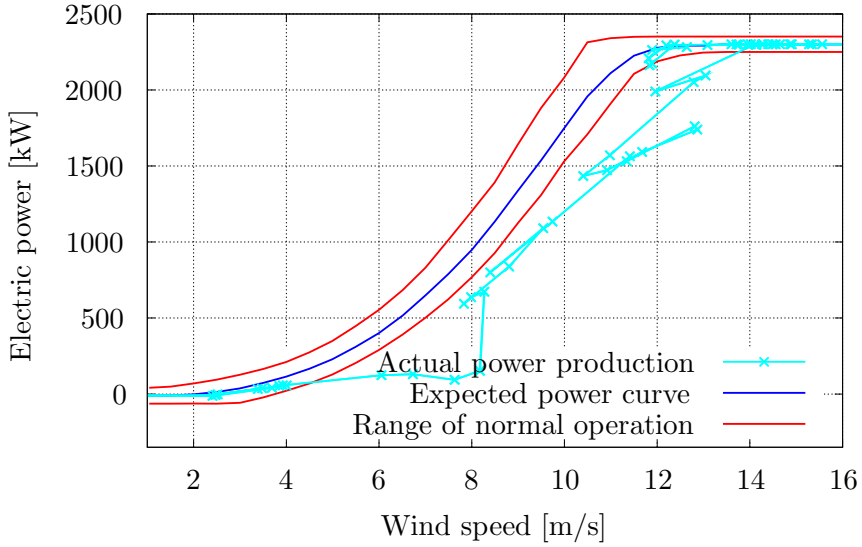

Fig. 8. Measured power production during the icing event of Jan. 8 (consecutive points are connected) can be seen to remain below the range of normal operation as the wind speed increases from near 0 up to rated speed. At about 20% over rated speed rated power is finally attained, and thereafter maintained.

3.3 Icing events and pitch angle

One item of interest observed during the second icing event was the turbine pitch angle. This is shown in Figure 9 and it can be seen that the pitch angle is first well below the normal range as rated wind speed is first reached. Thereafter the pitch angle remains 1-2 degrees below normal for the duration of the event. This shows that the turbine pitch control compensates for the lower aerodynamic performance of a slightly iced blade by increasing the pitch angle when above rated wind speed. This increased pitch angle means that the turbine blade and tower are likely subjected to greater than normal bending moments, but the analysis of such forces was beyond the scope of this work.

While it is far from a conclusive proof or verification of the model results, due to lack of data on the actual icing conditions during the period, and longer

icing duration than that modeled, these cases show that reductions in the power performance of actual turbines can be similar to the reductions in the modeled case. These cases thereby act to support the modeled results and give greater confidence in the modeling results. The modeled case represents an idealized case where constant icing conditions are maintained for one hour.

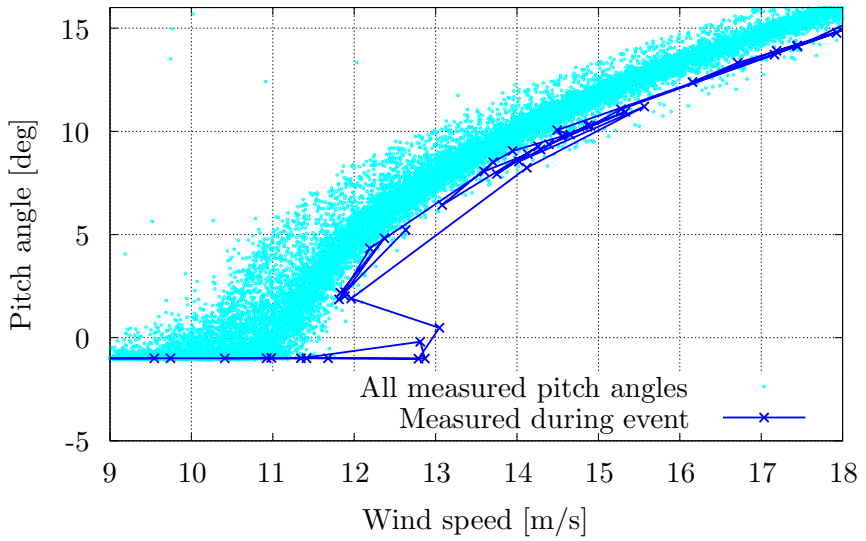

Fig. 9. Measured pitch curve during the icing event of Jan. 8 (consecutive points are connected) can be seen to be well below the range of normal operation as the wind speed increases above rated wind speed. It thereafter approaches normal pitch angle for higher wind speeds but continues to operate with a pitch angle of about 1-2 deg less than usual.

4 Conclusions

An icing event and the resulting effect on the power curve of the NREL 5 MW Baseline wind turbine was modeled and analyzed. The model results show a decrease in power production of 27% in region two.

The analysis of two icing events at Nygårdsfjell wind park and comparison with the modeled icing case for the NREL wind turbine indicate that actual reductions in power production can be greater than those modeled, which is reasonable when the duration of the modeled and actual icing events are compared. The results are deemed to correspond reasonably well with the observed effects and give confidence that the modeling methods used can be useful in estimating the effects of icing and exploring methods of reducing the adverse effects of icing.

It was seen from the operational data that a pitch controlled turbine can compensate for a partly iced blade in terms of power production, though this will have some effect on the loads the turbine is then subjected too. Future work regarding the effects of icing on fatigue of wind turbines should examine the effect of operating with this kind of changed pitch angle.

Modeling of more severe and longer duration icing cases would be interesting to confirm and expand on the results presented here.

Acknowledgments

Funding for this work was partly provided by The Research Council of Norway.

References

M. Virk, M.C. Homola, and P.J. Nicklasson. Effect of rime ice accretion on aerodynamic characteristics of wind turbine blade profiles. *Wind Engineering*, 34(2):207–218, 2010.

H. Seifert. Technical requirements for rotor blades operating in cold climate. In *Proceedings of the 2003 BOREAS VI Conference. Pyhätunturi, Finland*. Finnish Meteorological Institute, 2003.

H. Ganander and G. Ronsten. Design load aspects due to ice loading on wind turbine blades. In *Proceedings of the 2003 BOREAS VI Conference. Pyhätunturi, Finland*. Finnish Meteorological Institute, 2003.

G. Ronsten. Svenska erfarenheter av vindkraft i kallt klimat - nedisning, iskast och avisning. Elforsk rapport 04:13, 2004. (In Swedish).

W.J. Jasinski, S.C. Noe, M.S. Selig, and M.B. Bragg. Wind turbine performance under icing conditions. *Transactions of the ASME, Journal of solar energy engineering*, 120:60–65, 1998.

M.C. Homola, T. Wallenius, L. Makkonen, P.J. Nicklasson, and P.A. Sundsbø. The relationship between chord length and rime icing on wind turbines. *Wind Energy*, 2009. doi: 10.1002/we.383.

J. Jonkman, S. Butterfield, W. Musial, and G. Scott. Definition of a 5-MW reference wind turbine for offshore system development. Technical Report NREL/TP-500-38060, NREL, 2009. URL:http://www.nrel.gov/wind/pdfs/38060.pdf. Accessed: 2010-06-11. (Archived by WebCite at http://www.webcitation.org/5qPatf7uk).

P. Antikainen, S. Peuranen, T. Laakso, and E. Peltola. Modelling, verification and classification of ice loads in wind turbines. In *Proceedings of the BOREAS VI Conference*, 2003.

P. Antikainen and S. Peuranen. Ice loads, case study. In *Proceedings of the BOREAS V Conference*. Finnish Meteorological Institute, 2000.

Newmerical, 2010. URL:http://www.newmerical.com/index.php/products/fensap-ice-cfd-software/. Accessed: 2010-06-04. (Archived by WebCite at http://www.webcitation.org/5qF5VkNJ5).

H.J.T. Kooijman, C. Lindenburg, D. Winkelaar, and E.L. van der Hooft. Dowec 6 mw pre-design: Aero-elastic modelling of the dowec 6 mw pre-design in phatas. filename: 10046_009.pdf DOWEC-F1W2-HJK-01-046/9 public version, 2003. URL:http://www.ecn.nl/docs/dowec/10046_009.pdf. Accessed: 2011-01-04. (Archived by WebCite at http://www.webcitation.org/5vU1JUi35).

Ira H. Abbott and A. E. von Doenhoff. *Theory of Wing Sections: Including a Summary of Airfoil Data*. Dover Publications, 1959.

R. Van Rooij and W.A. Timmer. Roughness sensitivity considerations for thick rotor blade airfoils. *Journal of Solar Energy Engineering*, 125:468–478, 2003.

IEC 61400-12-1. *Wind turbines - Part 12-1: Power performance measurements of electricity producing wind turbines*. International Electrotechnical Commision, 2005.

MODELLING OF ICE INDUCED POWER LOSSES AND COMPARISON WITH OBSERVATIONS

Matthew C. Homola[a,b], Muhammad S. Virk[b], Per J. Nicklasson[b] and Per A. Sundsbø[b]

[a] – Nordkraft Produksjon, Narvik, Norway [b] - Narvik University College, Norway

1. Abstract

Some effects of ice on wind turbine blades are:

1. **Reduced energy production.** (Studied in this work.)
2. Overloading.
3. Increased fatigue
4. Dangers from ice shedding.

To better understand the effect of icing on energy production;

1. Ice accretion was modelled for a large pitch controlled wind turbine.
2. The effect on the power curve was calculated.
3. The changes in power production were compared with measurements from icing events at Nygårdsfjell windpark.

2. Modelling of icing

Ice accretion during a 1 hour icing event was modelled at five stations along the blade using the CFD solver FENSAP-ICE and the aerodynamic coefficients of the clean and iced profiles were determined using FENSAP.

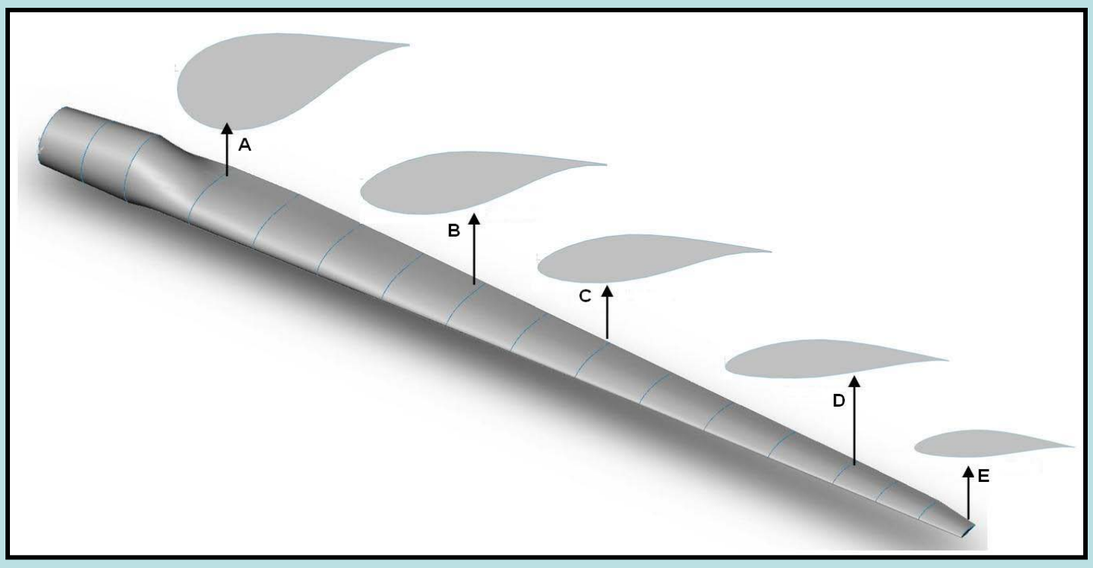

Sections where ice accretion was modelled.

Station	A	B	C	D	E
Radius (m)	13.25	33.75	41.95	54.25	63
Chord (m)	4.557	3.748	3.256	2.518	1.419

Blade element momentum (strip) theory was then used to calculate the power curves for the clean and iced cases (shown below).

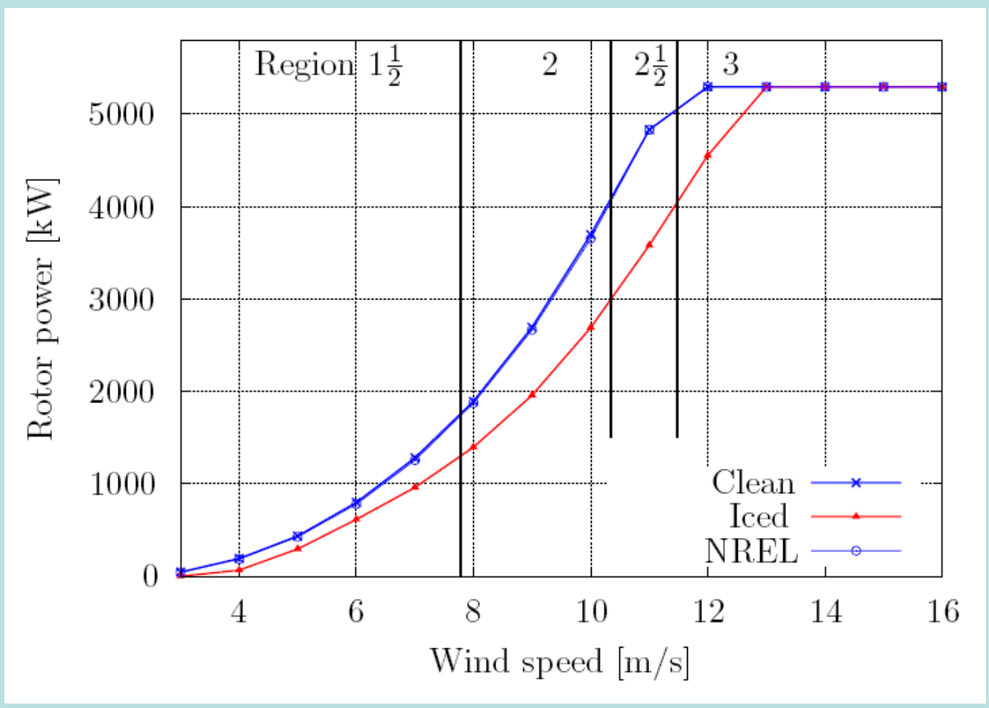

3. Observations

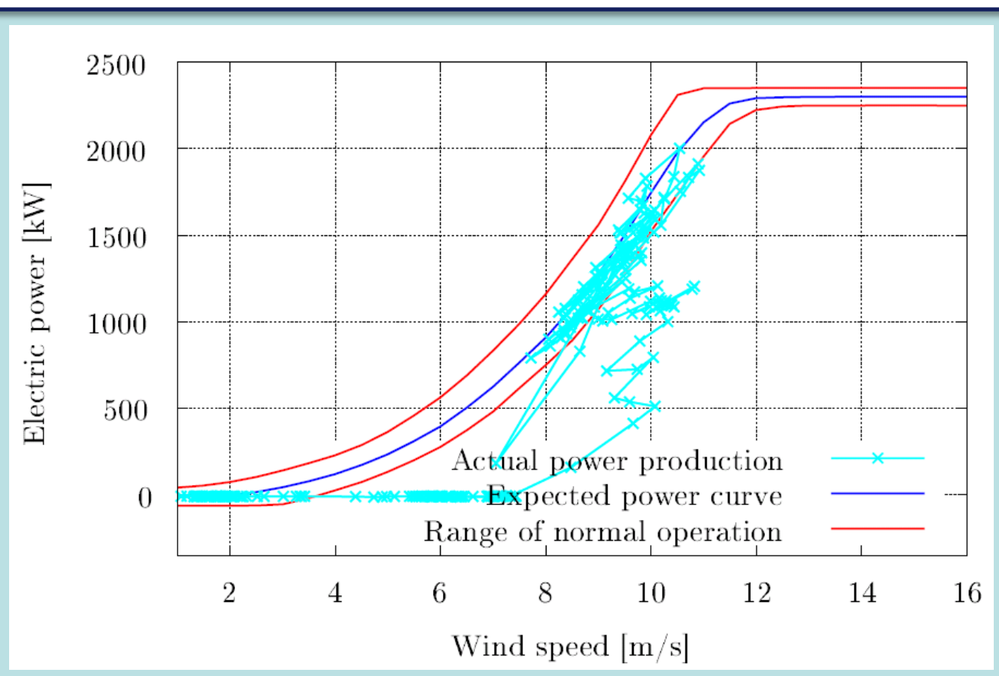

Ice event 1 – Ice accumulates with wind of about 8-10 m/s. Increasing ice leads to gradually lower production while wind speed is stable. Duration of over 12 hours. Production finally ceases with the iced turbine when the wind speed falls below about 8 m/s.

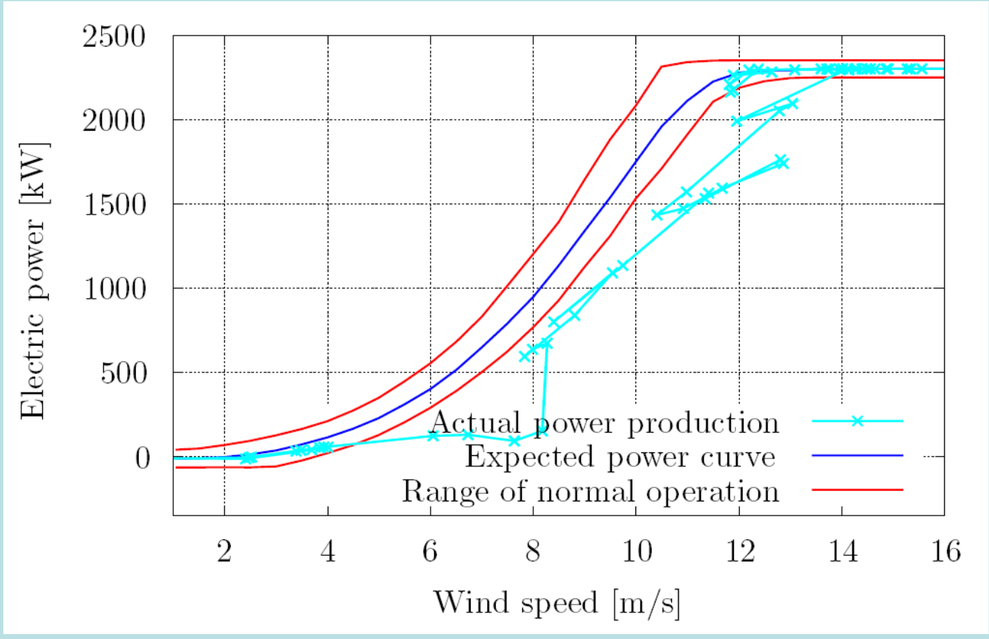

Ice event 2 – Wind speed increases during the event. Ice shedding is assumed to cause the vertical jump in production at around 8 m/s. Above rated wind speed the turbine is able to maintain rated power. Duration about 6 hours.

Lower than normal pitch angles were observed above rated wind speed as the turbine compensated for the lower aerodynamic performance of the blades.

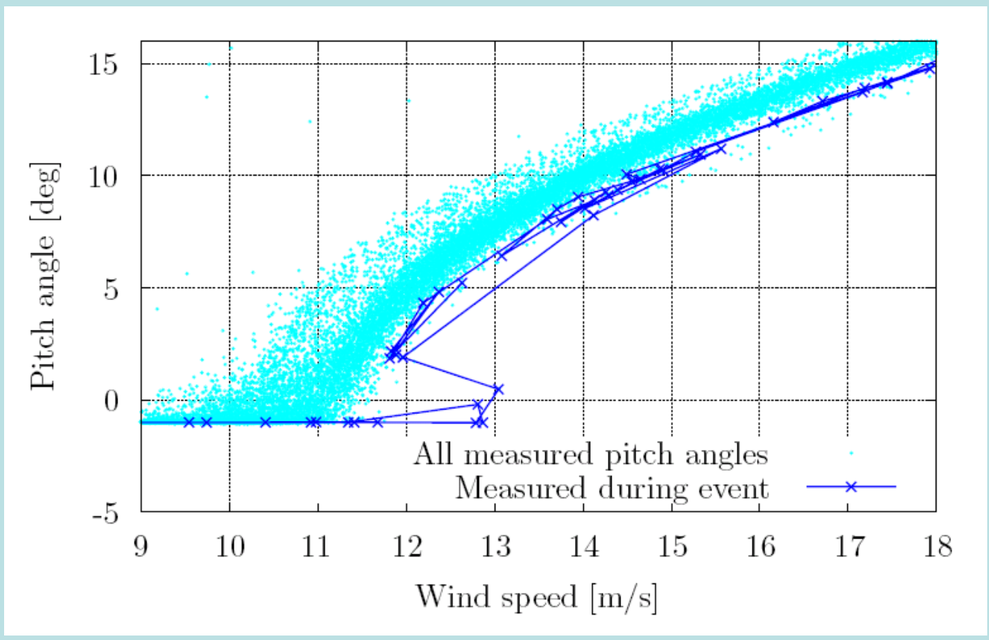

4. Conclusions

- Modelled icing losses were found to be about 27% in control region 2.
- Modelled reduction in icing corresponded reasonably well with the measured results.
- The observed events lasted much longer than the 1 hour modelled event.
- Observed power losses exceeded modelled power losses during parts of the events (likely due to the longer duration).
- Above rated wind speed the operating turbine was observed to compensate for the ice accretion by decreasing the pitch angle (this may have unintended consequences).